Effect of Drying on the Viscoelastic Response of a Dual-crosslinked PVA Hydrogel

Fan Cui, Jikun Wang, Alan Zehnder*, Chung-Yuen Hui

Sibley School of Mechanical and Aerospace Engineering, Cornell University, Ithaca, NY 14850, New York

Abstract

The effect of drying on the viscoelastic, tensile behavior of a dual cross-linked poly(vinyl alcohol)(PVA) hydrogel is studied experimentally. This gel contains about 90% water when fully hydrated and is highly stretchable. Using a microbalance with a density kit it is found that as the gel dries its volume shrinks in linear proportion to the mass. The impact of drying on the gel's mechanical properties is measured in uniaxial tension tests, which include loading-unloading tests at three different stretch rates, a complex loading history test consisting of two different loading segments and a stress-relaxation test. The resulting data show that the gel becomes much stiffer as the gel dries and that drier gels do not fully recover upon unloading. The viscoelastic response from specimens with different hydration levels can be described by a previously developed constitutive model of the gel. The results show that the constitutive model parameters are strongly dependent on hydration level.

Keywords: Hydration, Large strain, Uniaxial stress, Stiffness, Time dependent material, Constitutive model

1. Introduction

A hydrogel is essentially a network of polymer chains swollen in water. A wide range of hydrogels have been developed in the last decades [1–10] with intriguing properties such as the ability to self-heal, to undergo extremely large deformations and to show elastic or viscoelastic behaviors. The poly(vinyl alcohol) (PVA) gel studied here contains a large fraction of water (90%), is soft and can be highly elongated prior to failure. However, these properties will change greatly if the gel dries, even partially.

The gel we study consists of dual-crosslinked PVA polymer chains. Dual cross-linked means that the crosslinks are a mixture of physical (ionic) and chemical (covalent) bonds. The physical cross links can break and reform providing an energy dissipation mechanism that leads to viscoelastic behavior and well as a degree of self-healing [4, 6, 8–12]. The chemical cross-links do not break (until final failure) and impart long-term elasticity to the gel.

*Corresponding author.
Email address: atz2@cornell.edu (Alan Zehnder)

May 12, 2021

The idea of a dual cross-linked gel is motivated by the result that typical single cross-linked chemical hydrogels have poor mechanical strength, hence limiting their applications. To overcome this limitation, researchers have developed several new approaches to gel design to enhance the mechanical properties [13–15] . One method introduced by Gong et al. [16] is to introduce a double-network (DN) structure. In this DN gel, the gel contains two types of networks. The highly cross-linked first network has a relatively high Young's modulus but is rather brittle. The loosely cross-linked second network is highly extensible and prevents the formation of macroscopic cracks. However, this gel cannot fully recover to its original state after damage since the first sacrificial network is chemically cross-linked and cannot reattach after breaking [17] . Nevertheless, these DN gels still have good resistance to fatigue crack propagation [18]. Several groups of researchers also have synthesized highly stretchable and tough hydrogels by introducing non-covalent (physical) transient bonds as a sacrificial network [8, 9, 11, 12, 19, 20]. These physically cross-linked networks are reversibly broken during loading but they can reform and recover to their initial state after unloading and resting. Sun et al. [4] reported the synthesis of a tough polyampholyte (PA) hydrogel which has a fracture energy of about 4000 J/m^2 with only ionic bonds. This PA gel has a phase-separated structure composed of soft and stiff phases, with a structure length of $\sim$100 nm [21–24]. The ionic bonds have a wide distribution of strength and serve as sacrificial networks, enhancing fatigue life [25], fracture resistance and the self-healing behavior [26] of PA gels.

Being comprised mostly of water, hydrogels are prone to drying, leading to shrinkage and to changes of mechanical properties. The effect of hydration on hydrogels including drying and shrinkage has been studied by several researchers [27–36]. Some researchers focused on the behaviour of the hydrogel during the dehydration-rehydration cycle [27, 28] . Lee et al. [27] reported the shape stability of PVA hydrogels during the drying-rewetting cycle. Thomas et al. [28] found that a poly(vinyl alcohol) and poly(vinyl pyrrolidone)(PVA/PVP) gel shrinks in a dehydration-rehydration cycle and that the instantaneous compressive modulus increases. The more water it loses during the dehydration, the more the gel shrinks, and the more the modulus increases. This result is broadly consistent with available data. For example, Lee et al.'s work on PVA hydrogel [29] and Truong et al.'s work on rec1-resilin gel [30] both reported that the stiffness of their gel decreases as the hydration level increases. Gao and Gu [31] developed a relationship between the water content and elastic modulus for hydrated porous materials, showing that the modulus decreases with increasing hydration. Smyth et al. [32] reported that the stiffness of hydrogel films becomes lower when soaking in water. Zhang et al. [33] reported that for solvent treated VM-3-10-1 hydrogel, the modulus decreases as the gel becomes hydrated until the water content reaches 75% and then changes little as it reaches full hydration. There are some exceptions, e.g., Li et al. [34] found that for a bacterial cellulose and polyvinyl alcohol (BC/PVA) hydrogel, the compressive modulus of samples with PVA content less than 20% decreases compared to fully hydrated samples. The effect of hydration on the tensile strength of hydrogel films have been studied by Olivas et al. [35] and Pereira et al. [36] . They reported the tensile strength (breaking stress) of the film is lower when surface humidity is higher. Zhang et al. [33] reported that for the solvent treated VM-3-10-1 hydrogel the strain to failure increases as the water content increases.

While stiffness and tensile strength are important mechanical properties, they do not fully characterize the complex, time dependent behavior of viscoelastic gels. In this work, we focus on a dual-crosslinked PVA hydrogel developed by Mayumi et al. [10] containing both chemical and physical crosslinks. The chemical crosslinks form a permanent network. The physical crosslinks form a temporary network which can break and reattach. About 10% of the cross-links are chemical with the balance physical bonds. For a fully hydrated gel, we and our coworkers have established a constitutive model which accurately predicts its behavior [37, 38]. Liu at el. demonstrated that the mechanical properties of this PVA hydrogel over a range of temperatures can also described by this constitutive model [39]. Meacham at el. [40] performed a preliminary study of the effect of hydration on the tensile response of this PVA hydrogel. Here we investigate the effects of drying on the volume and time dependent constitutive response of the PVA hydrogel. We find that the constitutive model used for the fully hydrated gel can be used to quantify our experimental results and that changes in the model parameters provide insight into the role of hydration on the chemical and physical bonds.

2. Experiments

2.1. Material preparation

The experiments were performed on a dual-crosslinked PVA hydrogel which contained approximately 12% wt PVA and 88% wt an ionic solution. The details of the synthesis can be found in [10, 41] . Here we briefly summarize the procedures. There are three steps: making a 16% wt PVA solution, adding chemical cross-links, then adding physical crosslinks. First, PVA powder was added to distilled water at 5 °C. The mixture was stirred and heated to 95 °C to dissolve the PVA in the water. Then the PVA solution and glutaraldehyde cross-linker were mixed with hydrochloric acid at a pH of 1.4. The solution was injected into a mold and rested for 24 hours to form the chemical network. Finally, the chemically cross-linked gel was washed to neutralize the pH by soaking in distilled water for 24 hours. It was then soaked in an ionic solution made of water, sodium chloride and borax to form the ionic (physical) cross-links. After 3 to 4 days, the physical bonds have completely formed, and the gel is ready to be used in experiments.

2.2. Mass and volume measurement

The sample was then allowed to dry in lab air. Hydration levels were characterized by the amount of mass loss during drying. We also measured the mass-volume relationship at different hydration levels. The mass and volume of a fully hydrated sample were measured initially. We then measured its mass every 5-10 minutes until it reached 95%, 90%, 85%, 80%, 75%, 70%, 65% and 60% of the initial mass. For each of these hydration levels we also measured its volume. The mass was measured by a Mettler Toledo AG285 microbalance with an accuracy of 0.01 mg. The volume was measured by weighing the sample in air and in mineral oil using a density determination kit (DDK) on the microbalance. A schematic of the DDK is shown in figure 1. The red parts are connected to the microbalance plate so that we can measure the mass of the sample on the plate or in the basket. The black parts

hold up the beaker and are connected to the base of the balance, not to the balance plate itself.

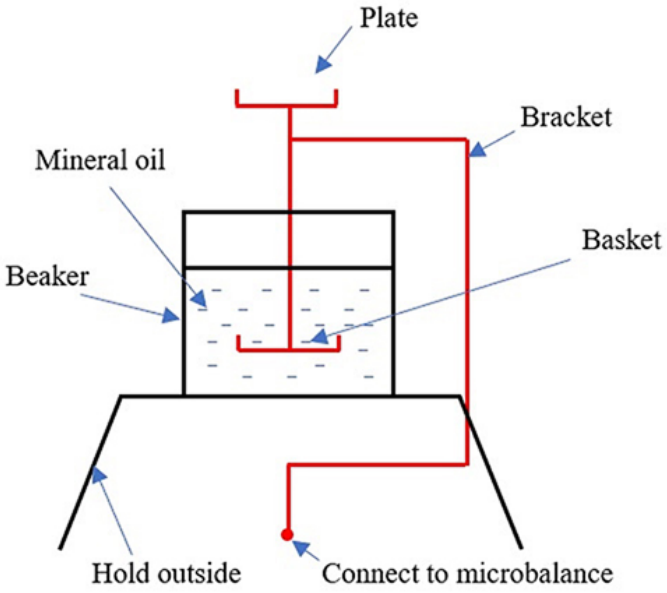

Figure 1: Schematics of the density determination kit.

First we measured the weight of the gel W_a on the plate in air. The mass of the sample in oil, W_o, is measured by placing it on the basket which is immersed in oil. By Archimedes principle, the buoyancy equals the volume of the sample (V_{sample}) multiplied by the density of the oil, ρ_{oil}, times the gravitational acceleration, g. The buoyancy is

$$F_b = W_a - W_o \tag{1a}$$

From

$$W_a - W_o = \rho_{oil} g V_{sample} \tag{1b}$$

we obtain

$$V_{sample} = \frac{W_a - W_o}{\rho_{oil} g} \tag{1c}$$

The density of the oil was measured by using a pipette to inject 1 mL of oil into a container on the microbalance. The reported density value is the average of three measurements.

2.3. Uniaxial tests

Mechanical tests were performed with a custom-built tensile tester [41] . A Zaber X-LSM200A-E03 translation stage was used to move the upper grip. An Interface SMT 1-1.1

load cell, with a capacity of 4.9 N (about 1.1 lbf), was used to measure the force. An OMEGA LD620 linear variable displacement transducer (LVDT) was used to measure displacement. The force and the displacement signal were recorded by a Keithley Model 2701 multiplexing digital voltmeter every 0.1 second. Samples were cut into strips 2 mm thick, 10 mm wide and clamped between a pair of sandpaper lined aluminum grips separated by a gauge length of 30 mm. All tests were performed in mineral oil to prevent the sample from further drying.

At each hydration level (100, 90, 80, 70 and 60%), six tests were performed. Tests were performed sequentially using the same sample for consistency. Between each test, the sample was allowed to relax for about 12 minutes to fully recover to its initial state. We carried out three different types of tests. For the fully hydrated gels (100% of mass), 90% and 80% mass gels, we first carried out cyclic tests where the sample was loaded to a stretch of $\lambda = 1.3$ at stretch rates of $\dot{\lambda} = 0.003/s,\ 0.01/s\ 0.03/s$ and then unloaded to $\lambda = 1$ at the same rate. Second, we carried out a complex loading history in which the sample was loaded to a stretch of $\lambda = 1.15$ at a rate of $\dot{\lambda} = 0.003/s$, held for 1 minute and then loaded to $\lambda = 1.3$ at $\dot{\lambda} = 0.03/s$, held for another 1 minute and then unloaded to $\lambda = 1$ at a rate of $\dot{\lambda} = 0.01/s$. Then the sample was loaded to $\lambda = 1.3$ at $\dot{\lambda} = 0.1/s$ and unloaded to $\lambda = 1$ at $\dot{\lambda} = 0.001/s$. This test is followed by a tensile-relaxation test at a maximum stretch of $\lambda = 1.3$ with an initial stretch rate of $\dot{\lambda} = 0.5/s$. For the 70% and 60% mass gels, the tensile relaxation test is performed first; followed by the complex loading history test and loading-unloading tests at different stretch rates.

Results are presented in terms of the nominal stress, σ i.e. applied force divided by the initial cross-sectional area of the sample. For the fully hydrated gel, the cross-sectional area was 2 mm $\times$ 10 mm. For the drying gels, we assume that the gel shrinks uniformly in all three dimensions, thus the cross-sectional area is calculated using $2\text{ mm} \times 10\text{ mm} \times (V\%)^{2/3}$, where $V\%$ is the volume percentage (volume after drying divided by initial volume at full hydration). The value of $V\%$ is found from the mass-volume relationship described below.

3. Results

3.1. Mass-volume relationship

The results of mass-volume experiments are shown in figure 2. The volume percentage (volume after drying divided by initial volume) decreases linearly with the mass percentage (mass after drying divided by initial mass). The data in figure 2 can be fit using $V\% = 1.03M\% - 3.04\%$, where $V\%$ is the volume percentage and $M\%$ is the mass percentage. This equation allows us to calculate the undeformed cross-section area of the gel at different hydration levels as described above.

3.2. Uniaxial tests

3.2.1. Test results

Figures 3a-d show the stress-strain curves for PVA hydrogels at different hydration levels for the cyclic test at different loading-unloading rates. Figure 3e shows the stress-strain curves for PVA hydrogels at different hydration levels for the complex-loading-history loading

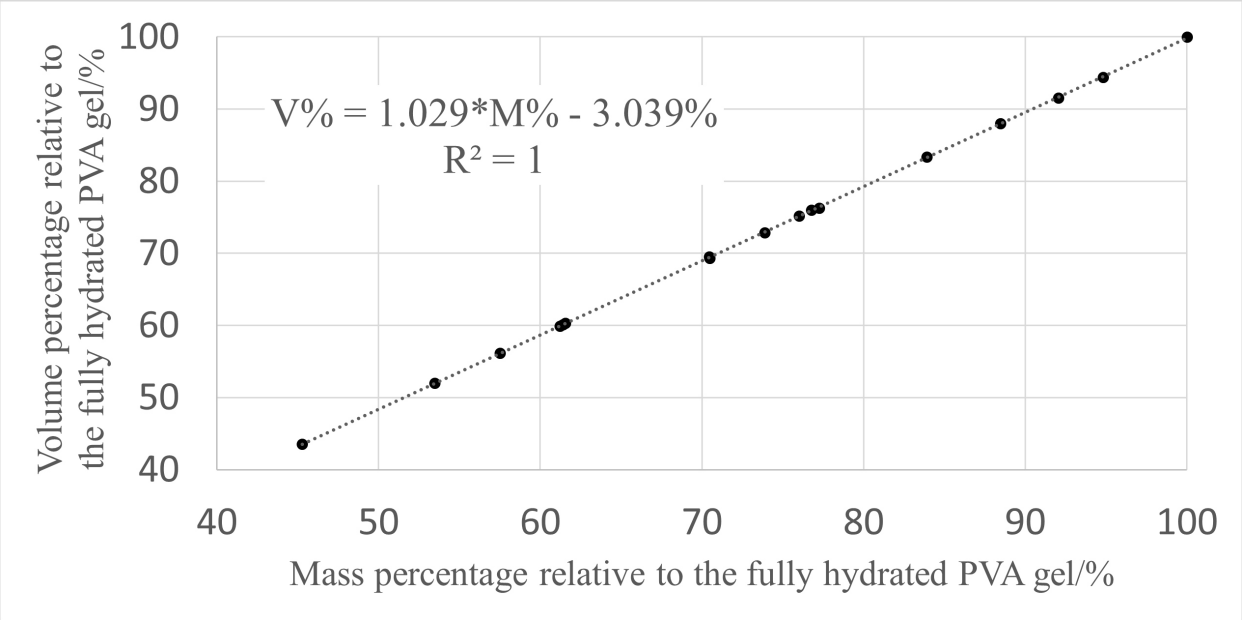

Figure 2: Mass-Volume relationship of PVA hydrogels during drying.

test. Figure 3f shows the stress-time curves for PVA hydrogels at different hydration levels in tensile-relaxation tests.

These figures show that for all stretch rates the stress is significantly higher as the gel dries. Figures 3a-e show that stress increases slowly at the initial stages of loading for the 70 and 60% hydration levels. Except for this initial dip, the maximum nominal stresses of the drier gels are higher, and across all tests we see that the gel stiffens as it dehydrates. It appears that that gel samples with mass percentages less than or equal to 70% did not had sufficient time to recover after the previous experiment. Indeed, we observed that these gels did not fully recover to their initial state after unloading to a stretch $\lambda = 1$ after the tensile-relaxation test, which indicates that in the drier gels the network may undergo permanent change during the loading. For fully hydrated hydrogels and 70% mass hydration level hydrogels, we did a recovery test. In this test, we first loaded the sample to stretch $\lambda = 1.3$ at stretch rate $\dot{\lambda} = 0.5/s$, then we held the sample at $\lambda = 1.3$ to perform a relaxation test. After 30 minutes of relaxation, we unloaded the sample to $\lambda = 1$ at rate $\dot{\lambda} = 0.001/s$. Then the sample was held for 4 hours to recover. We found that the 100% hydrated gels recovered fully after 700 s. However, the 70% gel did not fully recover even after 4 hours. The results of the recovery test are given in the supplemental material.

3.2.2. Review of constitutive model

The constitutive model of this PVA dual-crosslinked hydrogel was first developed by Long et al. and later modified by Guo et al. [37, 38]. Here we briefly review this model. The key assumptions are: Macroscopically the gel is isotropic and incompressible. It has two independent types of crosslinks. The chemical crosslinks form a permanent elastic network and do not break. The network formed by the physical crosslinks can break and reattach

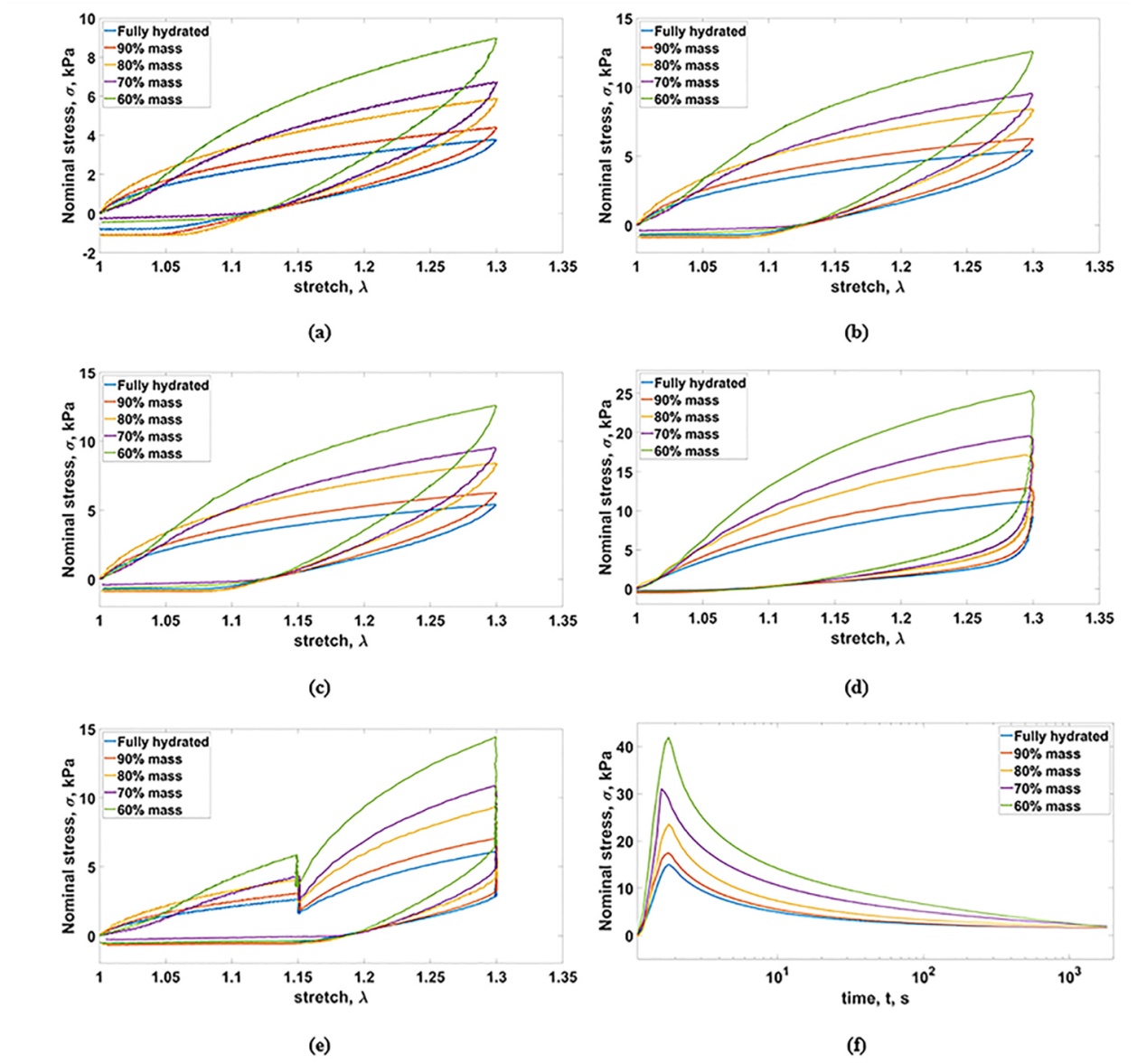

Figure 3: a) Nominal stress vs. stretch at five hydration states. Loading-unloading at stretch rate of $\dot{\lambda} = 0.003/s$. b) Nominal stress vs. stretch at five hydration states. Loading-unloading at stretch rate of $\dot{\lambda} = 0.01/s$. c) Nominal stress vs. stretch at five hydration states. Loading-unloading at stretch rate of $\dot{\lambda} = 0.03/s$. d) Nominal stress vs. stretch at five hydration states. Loading at stretch rate of $\dot{\lambda} = 0.1/s$ and unloading at stretch rate of $\dot{\lambda} = 0.001/s$. e) Nominal stress vs. stretch at five hydration states. A complex loading history (see text for description). f) Nominal stress vs. time in log scale for five hydration states in relaxation tests. Samples are loaded at $\dot{\lambda} = 0.5/s$ to a maximum stretch of 1.3.

with rates independent of strain. The breaking and reattaching reach an equilibrium soon after the gel is synthesized. A physical chain instantaneously releases all its strain energy when it breaks and it reattaches with zero strain energy. With these assumptions and using the neo-Hookean strain energy function, the nominal stress σ in a uniaxial tension test is related to the stretch λ by

$$\sigma = \mu\left(\rho + n\left(t\right)\right)\left[\lambda\left(t\right) - \frac{1}{\lambda^2\left(t\right)}\right] + \mu\overline{\gamma}_\infty \times \int_0^t \phi_B\left(\frac{t-\tau}{t_B}\right)\left[\frac{\lambda\left(t\right)}{\lambda^2\left(\tau\right)} - \frac{\lambda\left(\tau\right)}{\lambda^2\left(t\right)}\right]\mathrm{d}\,\tau \tag{2a}$$

where
μ is the small strain shear modulus of neo-Hookean model.
ρ is the molar fraction of the chemical crosslinks.
$\overline{\gamma}_\infty$ is the steady state reattachment rate of the physical chains, i.e., molar fraction of the physical chains reattached per unit time, hence $\overline{\gamma}_\infty d\tau$ is the number of newly reattached physical chains,

The integrand

$$\left(\overline{\gamma}_\infty d\tau\right)\phi_B\left(\frac{t-\tau}{t_B}\right) = \overline{\gamma}_\infty\left[\left(1 + \left(\alpha_B - 1\right)\frac{t}{t_B}\right)^{\frac{1}{1-\alpha_B}}\right]d\tau \tag{2b}$$

is the number of chains that healed between τ and $\tau + d\tau$ and survives until t, where t_B is the characteristic time for breaking; $2 > \alpha_B > 1$ is a material constant that specifies the rate of decay of ϕ_B.

$n\left(t\right)$ is the molar fraction of physical bonds at $t = 0$ and still attached at t ; it is given by

$$n\left(t\right) = \overline{\gamma}_\infty \int_{-\infty}^0 \phi_B\left(\frac{t-\tau}{t_B}\right)\mathrm{d}\,\tau = \overline{\gamma}_\infty \frac{t_B}{2-\alpha_B}\left(1 + \left(\alpha_B - 1\right)\frac{t}{t_B}\right)^{\frac{2-\alpha_B}{1-\alpha_B}} \tag{2c}$$

In this model, the constitutive relationship is completely specified by four independent material parameters:$\mu\rho$, $\mu\overline{\gamma}_\infty$, α_B and t_B. For physical understanding, $\mu\rho$ corresponds to the shear modulus of the network crosslinked only by the chemical crosslinks. $\mu\overline{\gamma}_\infty$ can be roughly thought of as a parameter measuring how stresses increase with the number of reattached physical chains per unit time. $2 > \alpha_B > 1$ controls the average survival time of a newly attached transient bond and t_B is the characteristic time for breaking.

3.2.3. Determination of material parameters

In our previous work, we determined the four material parameters mainly using the stress relaxation test parameters [38]. We then used these parameters and equation (2c) to predict the stress-stretch curve for cyclic test. These predicted stress strain curves are then compared with experiments and manually adjusted to proivde a good overall fit. Here we accelerated the fitting process using a machine learning algorithm (MLA) to determine

these material parameters. Details of this method can be found in our recent paper [42] and a brief summary of the method is given in the supplemental material. We use all the six experiments to fit the data of 100%, 90%, 80% mass hydration levels. We use only the first 200 seconds of the relaxation tests to fit the data for the 70% and 60% mass hydration level hydrogels since the initial dip in stress that occurs in the cyclic loading tests cannot be fit by the model.

The parameters obtained using our MLA are shown in table 1.

Table 1: Data fitting results for PVA hydrogels atdifferent hydration levels.

Hydration	$\mu\rho$ (kPa)	α_{B}	t_{B} (s)	$\mu\overline{\gamma}_{\infty}$ (kPa/s)	$\frac{\mu\overline{\gamma}_{\infty}\mathrm{t}_{\mathrm{B}}}{2-\alpha_{\mathrm{B}}}$ (kPa)
100% mass	2.347	1.634	0.4618	19.91	25.15
90% mass	2.567	1.633	0.4335	26.72	31.53
80% mass	2.640	1.664	0.4250	31.62	40.05
70% mass	2.994	1.674	0.3383	48.76	50.62
60% mass	3.439	1.687	0.2338	101.2	75.55

Comparisons of model and experiments are shown in figures 4-8. Figures 4-6 show that there is excellent agreement between experiments with different loading histories and constitutive model as long as drying is not so severe that permanent deformation is experienced by the samples. For the 60% and 70% hydrated gels, our model fails to predict the cyclic tests and the complex loading test. As shown in section 3.2.1, for samples at 70% and 60% mass, the stress increases slowly at the initial part of loading for the loading-unloading tests. This is likely due to permanent deformation remaining after the relaxation test. For these samples, our constitutive model does not work well. Hence, we use only the first 200 seconds of relaxation test to compare with the model (recall that the relaxation test was performed on a virgin sample at 70% and 60% mass hydration level).

4. Discussion

4.1. Effect of dehydration

4.1.1. Volume change

In section 3.1 and figure 2, we showed that the volume percentage (volume after drying divided by initial volume) decreases linearly with the mass percentage (mass after drying divided by initial mass). The relationship can be described by equation $V\% = 1.03M\% - 3.04\%$, where $V\%$ is the volume percentage and $M\%$ is the mass percentage. The equation can also be written as,

$$\frac{V_D}{V_I} = 1.03 \times \frac{M_D}{M_I} - 0.0304 \tag{3a}$$

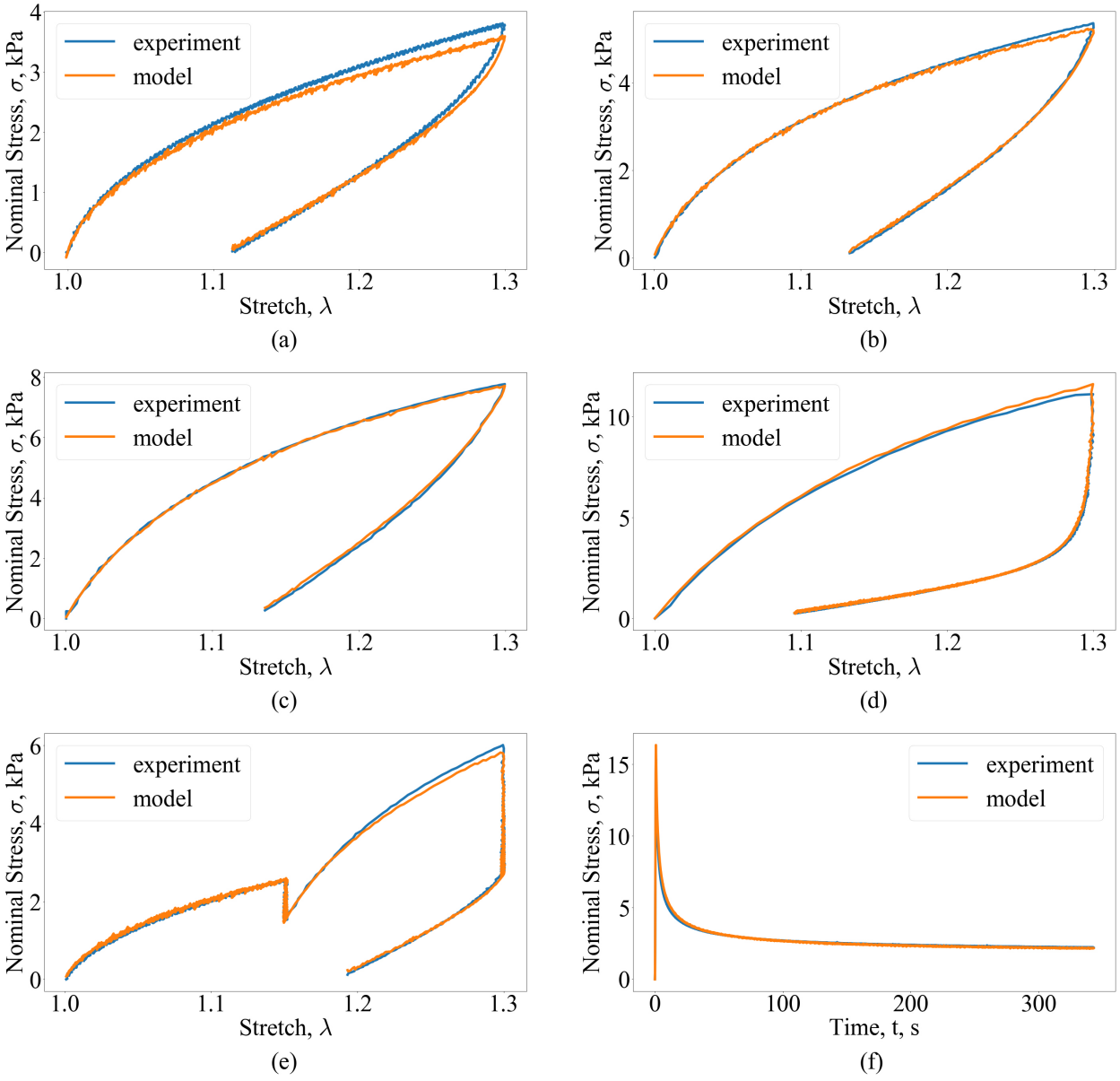

Figure 4: Comparsion between model and experiments for fully hydrated(100% mass) PVA hydrogel. Nominal Stress vs. Stretch for (a) Loading-unloading to stretch $\lambda = 1.3$ at stretch rate 0.003/s. (b) Loading-unloading to stretch $\lambda = 1.3$ at stretch rate 0.01/s. (c) Loading-unloading to stretch $\lambda = 1.3$ at stretch rate 0.03/s. (d) Loading to stretch $\lambda = 1.3$ at stretch rate 0.1/s and unloading at stretch rate 0.001/s. (e) A complex loading history which was mentioned above. (f) Nominal Stress vs. Time for loading at stretch rate 0.5/s to a stretch of 1.3 and then holding as the stress relaxes.

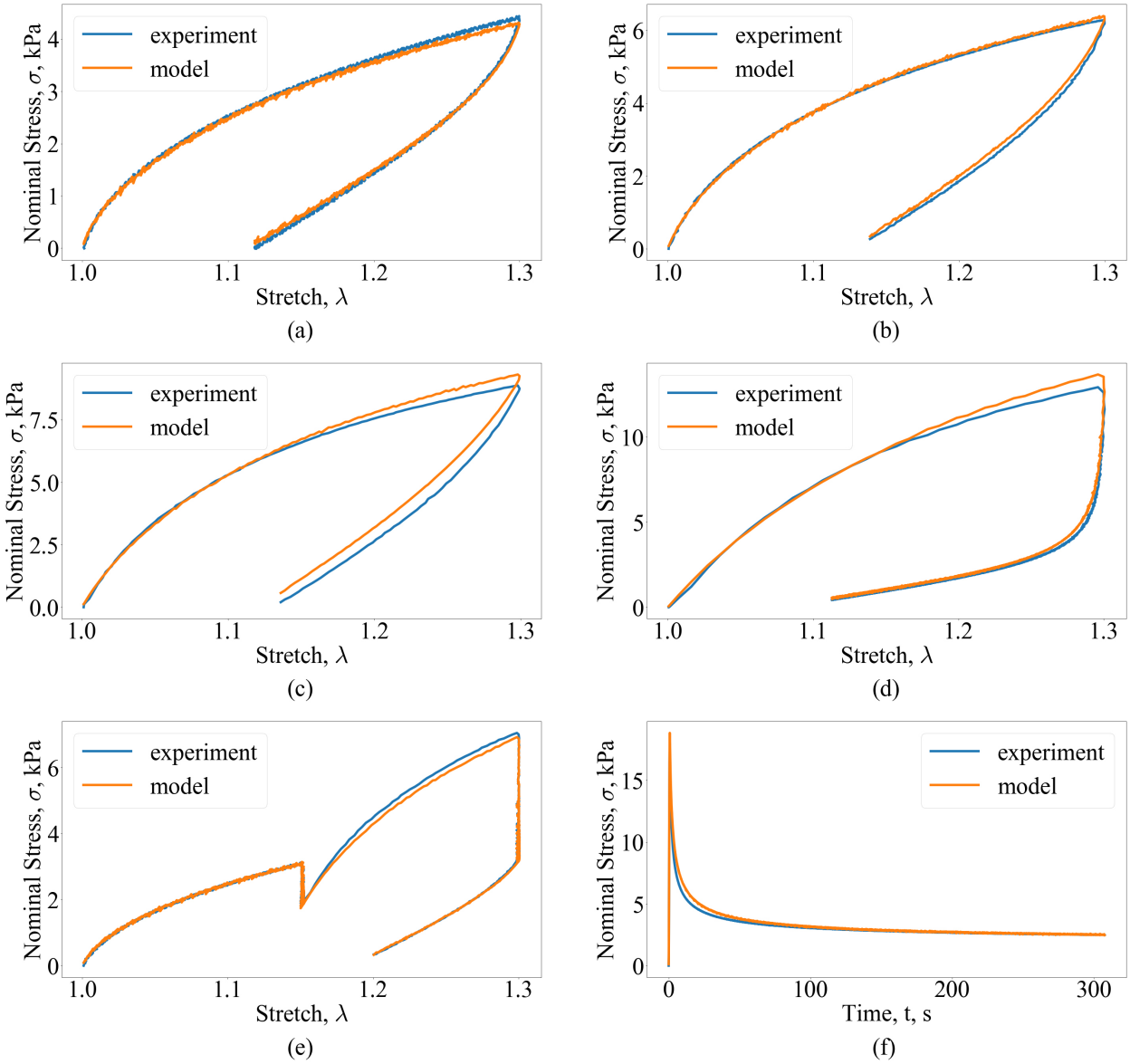

Figure 5: Comparsion between model and experiments for 90% mass PVA hydrogel. Nominal Stress vs. Stretch for (a) Loading-unloading to stretch $\lambda = 1.3$ at stretch rate 0.003/s. (b) Loading-unloading to stretch $\lambda = 1.3$ at stretch rate 0.01/s. (c) Loading-unloading to stretch $\lambda = 1.3$ at stretch rate 0.03/s. (d) Loading to stretch $\lambda = 1.3$ at stretch rate 0.1/s and unloading at stretch rate 0.001/s. (e) A complex loading history which was mentioned above. (f) Nominal Stress vs. Time for loading at stretch rate 0.5/s to a stretch of 1.3 and then holding as the stress relaxes.

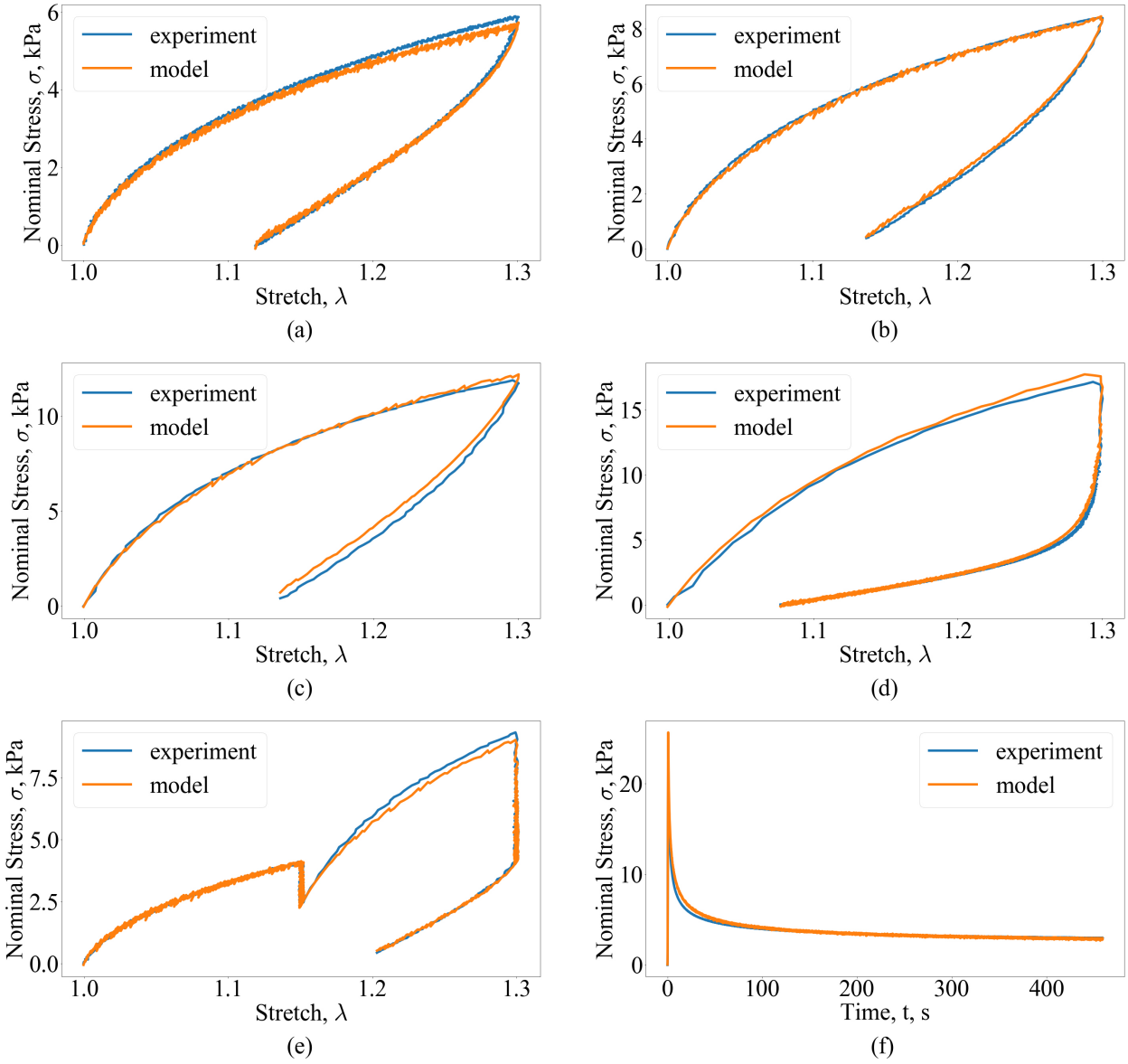

Figure 6: Comparsion between model and experiments for 80% mass PVA hydrogel. Nominal Stress vs. Stretch for (a) Loading-unloading to stretch $\lambda = 1.3$ at stretch rate 0.003/s. (b) Loading-unloading to stretch $\lambda = 1.3$ at stretch rate 0.01/s. (c) Loading-unloading to stretch $\lambda = 1.3$ at stretch rate 0.03/s. (d) Loading to stretch $\lambda = 1.3$ at stretch rate 0.1/s and unloading at stretch rate 0.001/s. (e) A complex loading history which was mentioned above. (f) Nominal Stress vs. Time for loading at stretch rate 0.5/s to a stretch of 1.3 and then holding as the stress relaxes.

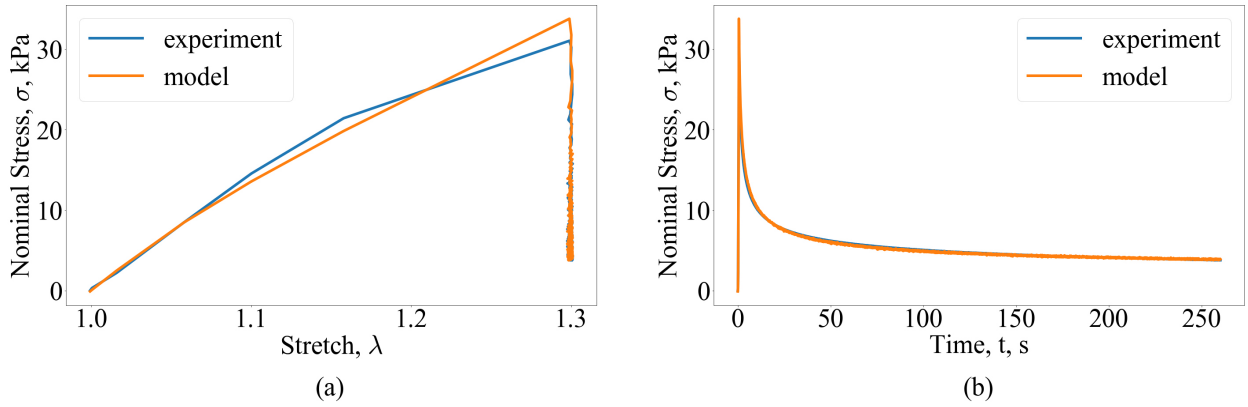

Figure 7: Comparsion between model and experiments for 70% mass PVA hydrogel. (a) Nominal Stress vs. Stretch for loading at stretch rate 0.5/s to a stretch of 1.3 and then holding as the stress relaxes. (b) Nominal Stress vs. Time for loading at stretch rate 0.5/s to a stretch of 1.3 and then holding as the stress relaxes.

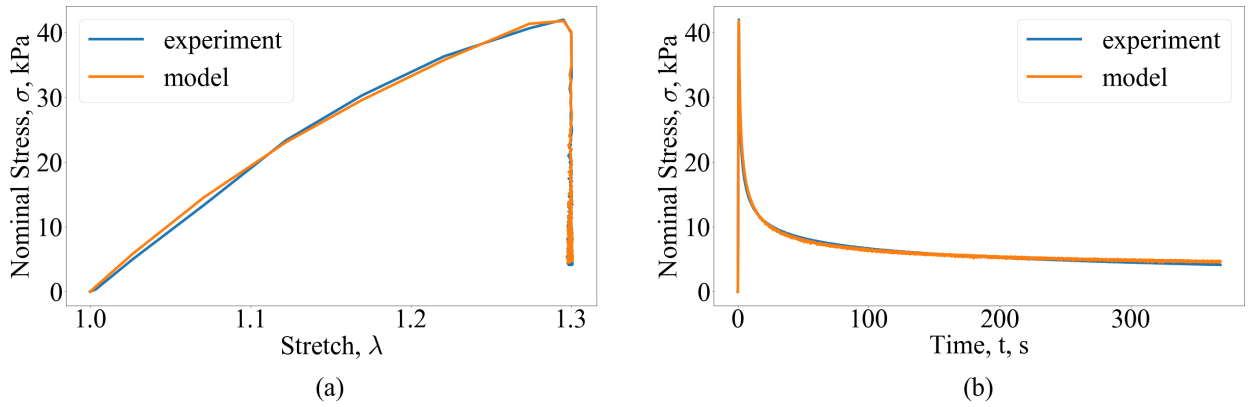

Figure 8: Comparsion between model and experiments for 60% mass PVA hydrogel. (a) Nominal Stress vs. Stretch for loading at stretch rate 0.5/s to a stretch of 1.3 and then holding as the stress relaxes. (b) Nominal Stress vs. Time for loading at stretch rate 0.5/s to a stretch of 1.3 and then holding as the stress relaxes.

where V_D is the volume after drying, V_I is the initial volume, M_D is the mass after drying and M_I is the initial mass. Rounding the above, equation (3a) can be written as

$$\frac{V_D}{V_I} - 1 = 1.03\left(\frac{M_D}{M_I} - 1\right) \tag{3b}$$

or

$$\frac{M_I}{V_I} = 1.03 \times \frac{M_I - M_D}{V_I - V_D} \tag{3c}$$

The left side of the equation is the density of the initial sample which is fully hydrated. In our experiment, the measured density of the fully hydrated PVA hydrogel is 1.006 g/cm^3. So we

can obtain that $(M_I - M_D)/(V_I - V_D) = 0.977 g/cm^3$. We know that $M_I - M_D$ is the mass loss of water during drying. If we consider the water and polymer network as two separate parts, then $(M_I - M_D)/(V_I - V_D)$ should be exactly the density of the water, which is 1 g/cm^3. Therefore, the results show that while the volume loss of the PVA gel during drying is mainly caused by water loss, additional shrinkage occurs due to other mechanisms.

4.1.2. Mechanical properties

According to our constitutive model [38], at long time (when the physical network does not carry any load), the behavior of the nominal stress $\sigma \equiv \sigma_\infty$ in a relaxation test of stretch λ_0 is

$$\sigma_\infty = \mu\rho\left(\lambda_0 - \frac{1}{\lambda_0^2}\right) \tag{4a}$$

Thus, the parameter $\mu\rho$ is the equilibrium modulus which is governed by the permanent (chemical) network.

The initial slope of the stress versus time curve in a tensile relaxation test is

$$\lim_{t\to 0}\frac{\sigma}{t} = 3\dot{\lambda}\left(\mu\rho + \frac{\mu\overline{\gamma}_\infty t_B}{2-\alpha_B}\right) \tag{4b}$$

The parameter $\overline{\gamma}_\infty \mathrm{t_B}/(2-\alpha_\mathrm{B})$ represents the molar fraction of connected physical chains and hence $\mu\overline{\gamma}_\infty \mathrm{t_B}/(2-\alpha_\mathrm{B})$ can be interpreted as the instantaneous modulus associated with the physical (transient) network. Figure 9 shows the change of both $\mu\rho$ and $\mu\overline{\gamma}_\infty \mathrm{t_B}/(2-\alpha_\mathrm{B})$ with respect to hydration level.

From table 1 or figure 9, $\mu\rho$ increases by about 47% when the PVA gel dries from 100% to 60% mass. This means the chemical network is stiffer and carries more load when the gel dries. Table 1 shows that α_B changes little when the gel dehydrates while t_B decreases and $\mu\overline{\gamma}_\infty$ increases. This suggests physical bonds break and reattach faster when the gel loses water. From the last column in table 1, and figure 9, $\mu\overline{\gamma}_\infty \mathrm{t_B}/(2-\alpha_\mathrm{B})$, increases by a factor or three when the PVA gel dries from 100% to 60% mass. Thus, the short time modulus of the gel, which involves both the physical bonds and chemical network, increases strongly with drying. From table 1 and figure 9, we see that the drier PVA gels are stiffer and hat the water content has a much more significant influence on the physical crosslinks than the chemical crosslinks as evidenced by the far greater increase in $\mu\overline{\gamma}_\infty \mathrm{t_B}/(2-\alpha_\mathrm{B})$ relative to $\mu\rho$. Physically, the loss of water will enhance the ion concentration inside the hydrogel, reduce screening and making the ionic interaction more active and stronger. Hence, the hydration level should have a more significant influence on the physical interaction than the permanent chemical network. This is consistent with our experimental results.

4.2. Limitations of the model

For the 70% and 60% mass PVA dual-crosslinked hydrogels, our constitutive model cannot totally explain the experimental results. These gels do not fully recover to their initial state after the tensile-relaxation test, which indicates that the network may have suffered

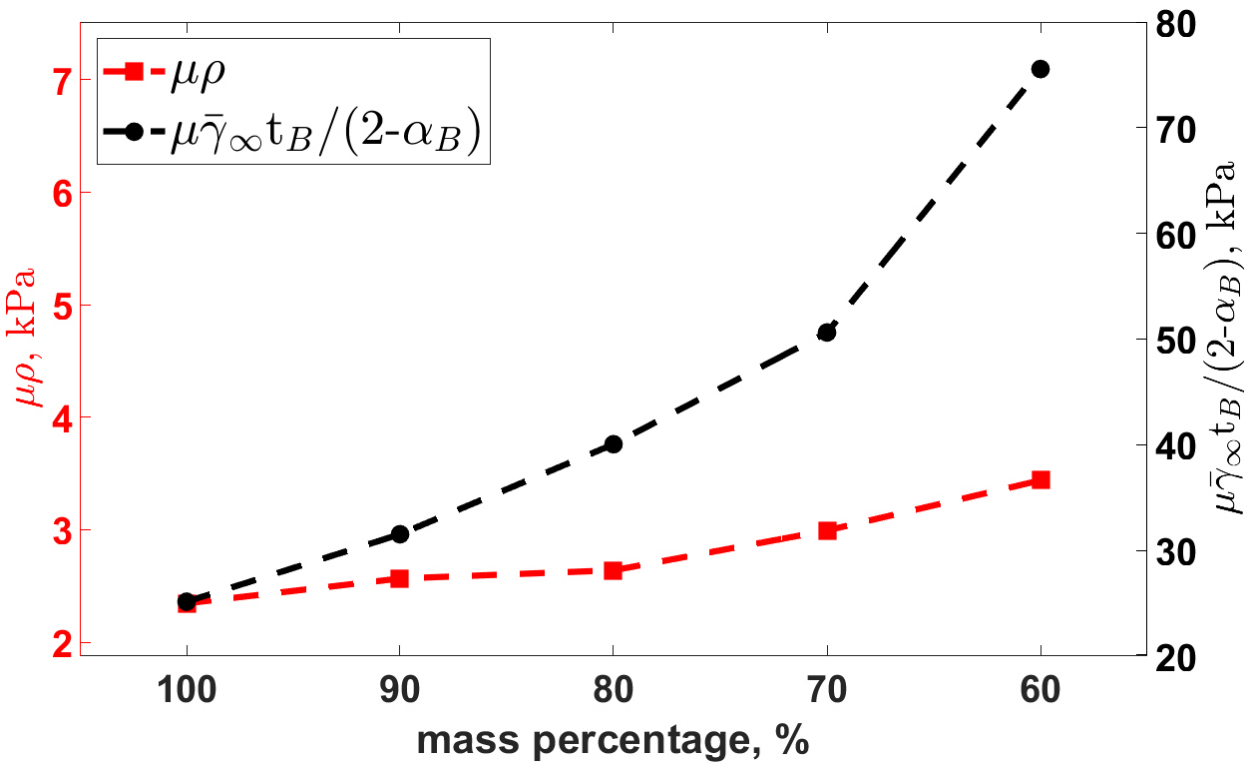

Figure 9: The change of $\mu\rho$ and $\mu\bar{\gamma}_\infty t_B/(2-\alpha_B)$ with respect to the hydration level.

permanent change during the test. In the supplemental material, we compare the results of the recovery test for fully hydrated hydrogels and 70% mass hydration level hydrogels. Our result shows that the 70% mass gels have a large residual stress after unloading to their initial length and that this residual stress persists even after the gel is rested for several hours. Figure 3f shows that the nominal stress in tensile-relaxation test after 1000 second drops rapidly for the 70% and 60% mass gels and the stress eventually becomes smaller than the stress of gels at higher hydration levels (please see the zoom-in figure for the long-time stresses for these cases in supplemental material). This result contradicts our model which predicts that at long times, physical bonds do not carry load in a relaxation test and the stress should plateau at $\mu\rho\left(\lambda_0-\lambda_0^{-2}\right)$, where λ_0 is the imposed stretch. Since $\mu\rho$ is the modulus associated with the chemical crosslinks, which increases as the gel dries (see table 1), the plateau stress should be higher as the gels dry instead of lower. Likewise, the stress of 60% mass hydration level hydrogel did not reach a plateau within our time of observation. Recall that we fit the relaxation experiment using first 200 seconds of data and it fits well for the loading part and the start of the relaxation part. These results, i.e., the rapid drop in stress and the lower long-time stress for gels at 70% and 60% mass hydration level suggest some permanent change to the chemical network during deformation of the 60% and 70% mass gels. Thus, our constitutive model does not totally explain the last part of the relaxation test as well as the tension tests performed following the relaxation tests. This is a subject for future work.

5. Conclusion

In summary, we present experimental results on how drying changes the mechanical properties of a PVA dual-crosslinked hydrogel. We performed six experiments on this hydrogel with different strain histories under uniaxial stress state and use a new fitting method which is based on Gaussian Process Machine learning to obtain the material parameters for our constitutive model. For gels that are moderately hydrated, our constitutive model is shown to be highly accurate and able to predict complex loading behavior. Our model shows both the physical and chemical network stiffens as the gel dries. However, drying stiffens the physical network much more than the chemical network.

Acknowledgements

This material is based upon work supported by the National Science Foundation, under Grant No. CMMI-1903308.

References

[1] S. Mondal, S. Das, A. K. Nandi, A review on recent advances in polymer and peptide hydrogels, Soft Matter 16 (6) (2020) 1404–1454. doi:10.1039/C9SM02127B.

[2] H. G. Schild, Poly(N-isopropylacrylamide): experiment, theory and application, Progress in Polymer Science 17 (2) (1992) 163–249. doi:https://doi.org/10.1016/0079-6700(92)90023-R.

[3] K. Imato, M. Nishihara, T. Kanehara, Y. Amamoto, A. Takahara, H. Otsuka, Self-Healing of Chemical Gels Cross-Linked by Diarylbibenzofuranone-Based Trigger-Free Dynamic Covalent Bonds at Room Temperature, Angewandte Chemie International Edition 51 (5) (2012) 1138–1142. doi:https://doi.org/10.1002/anie.201104069.

[4] T. L. Sun, T. Kurokawa, S. Kuroda, A. B. Ihsan, T. Akasaki, K. Sato, M. A. Haque, T. Nakajima, J. P. Gong, Physical hydrogels composed of polyampholytes demonstrate high toughness and viscoelasticity, Nature Materials 12 (10) (2013) 932–937. doi:10.1038/nmat3713.
URL https://dx.doi.org/10.1038/nmat3713

[5] H. J. Zhang, T. L. Sun, A. K. Zhang, Y. Ikura, T. Nakajima, T. Nonoyama, T. Kurokawa, O. Ito, H. Ishitobi, J. P. Gong, Tough Physical Double-Network Hydrogels Based on Amphiphilic Triblock Copolymers, Advanced Materials 28 (24) (2016) 4884–4890. doi:https://doi.org/10.1002/adma.201600466.

[6] Y. Hu, Z. Du, X. Deng, T. Wang, Z. Yang, W. Zhou, C. Wang, Dual Physically Cross-Linked Hydrogels with High Stretchability, Toughness, and Good Self-Recoverability, Macromolecules 49 (15) (2016) 5660–5668. doi:10.1021/acs.macromol.6b00584.

[7] X. Le, W. Lu, J. Zheng, D. Tong, N. Zhao, C. Ma, H. Xiao, J. Zhang, Y. Huang, T. Chen, Stretchable supramolecular hydrogels with triple shape memory effect, Chem. Sci. 7 (11) (2016) 6715–6720. doi:10.1039/C6SC02354A.

[8] J.-Y. Sun, X. Zhao, W. R. K. Illeperuma, O. Chaudhuri, K. H. Oh, D. J. Mooney, J. J. Vlassak, Z. Suo, Highly stretchable and tough hydrogels, Nature 489 (7414) (2012) 133–136. doi:10.1038/nature11409.
URL https://dx.doi.org/10.1038/nature11409

[9] L. Carlsson, S. Rose, D. Hourdet, A. Marcellan, Nano-hybrid self-crosslinked PDMA/silica hydrogels, Soft Matter 6 (15) (2010) 3619–3631. doi:10.1039/C0SM00009D.

[10] K. Mayumi, A. Marcellan, G. Ducouret, C. Creton, T. Narita, Stress–Strain Relationship of Highly Stretchable Dual Cross-Link Gels: Separability of Strain and Time Effect, ACS Macro Letters 2 (12) (2013) 1065–1068. doi:10.1021/mz4005106.
URL https://dx.doi.org/10.1021/mz4005106

[11] S. Rose, A. Dizeux, T. Narita, D. Hourdet, A. Marcellan, Time Dependence of Dissipative and Recovery Processes in Nanohybrid Hydrogels, Macromolecules 46 (10) (2013) 4095–4104. doi:10.1021/ma400447j.
[12] K. J. Henderson, T. C. Zhou, K. J. Otim, K. R. Shull, Ionically Cross-Linked Triblock Copolymer Hydrogels with High Strength, Macromolecules 43 (14) (2010) 6193–6201. doi:10.1021/ma100963m.
[13] Y. Okumura, K. Ito, The Polyrotaxane Gel: A Topological Gel by Figure-of-Eight Cross-links, Advanced Materials 13 (7) (2001) 485–487. doi:10.1002/1521-4095(200104)13:7<485::aid-adma485>3.0.co;2-t.
URL https://dx.doi.org/10.1002/1521-4095(200104)13:7<485::aid-adma485>3.0.co;2-t
[14] T. Sakai, T. Matsunaga, Y. Yamamoto, C. Ito, R. Yoshida, S. Suzuki, N. Sasaki, M. Shibayama, U. il Chung, Design and Fabrication of a High-Strength Hydrogel with Ideally Homogeneous Network Structure from Tetrahedron-like Macromonomers, Macromolecules 41 (14) (2008) 5379–5384. doi:10.1021/ma800476x.
URL https://dx.doi.org/10.1021/ma800476x
[15] K. Haraguchi, T. Takehisa, S. Fan, Effects of Clay Content on the Properties of Nanocomposite Hydrogels Composed of Poly(N-isopropylacrylamide) and Clay, Macromolecules 35 (27) (2002) 10162–10171. doi:10.1021/ma021301r.
[16] J. P. Gong, Y. Katsuyama, T. Kurokawa, Y. Osada, Double-Network Hydrogels with Extremely High Mechanical Strength, Advanced Materials 15 (14) (2003) 1155–1158. doi:10.1002/adma.200304907.
URL https://dx.doi.org/10.1002/adma.200304907
[17] R. E. Webber, C. Creton, H. R. Brown, J. P. Gong, Large Strain Hysteresis and Mullins Effect of Tough Double-Network Hydrogels, Macromolecules 40 (8) (2007) 2919–2927. doi:10.1021/ma062924y.
URL https://dx.doi.org/10.1021/ma062924y
[18] W. Zhang, X. Liu, J. Wang, J. Tang, J. Hu, T. Lu, Z. Suo, Fatigue of Double-Network Hydrogels, Engineering Fracture Mechanics 187 (2018) 74–93.
[19] W.-C. Lin, W. Fan, A. Marcellan, D. Hourdet, C. Creton, Large Strain and Fracture Properties of Poly(dimethylacrylamide)/Silica Hybrid Hydrogels, Macromolecules 43 (5) (2010) 2554–2563. doi:10.1021/ma901937r.
[20] M. A. Haque, T. Kurokawa, G. Kamita, J. P. Gong, Lamellar Bilayers as Reversible Sacrificial Bonds To Toughen Hydrogel: Hysteresis, Self-Recovery, Fatigue Resistance, and Crack Blunting, Macromolecules 44 (22) (2011) 8916–8924. doi:10.1021/ma201653t.
[21] K. Cui, T. L. Sun, X. Liang, K. Nakajima, Y. N. Ye, L. Chen, T. Kurokawa, J. P. Gong, Multiscale Energy Dissipation Mechanism in Tough and Self-Healing Hydrogels, Phys. Rev. Lett. 121 (18) (2018) 185501. doi:10.1103/PhysRevLett.121.185501.
[22] K. Cui, Y. N. Ye, T. L. Sun, L. Chen, X. Li, T. Kurokawa, T. Nakajima, T. Nonoyama, J. P. Gong, Effect of Structure Heterogeneity on Mechanical Performance of Physical Polyampholytes Hydrogels, Macromolecules 52 (19) (2019) 7369–7378. doi:10.1021/acs.macromol.9b01676.
[23] K. Cui, Y. N. Ye, T. L. Sun, C. Yu, X. Li, T. Kurokawa, J. P. Gong, Phase Separation Behavior in Tough and Self-Healing Polyampholyte Hydrogels, Macromolecules 53 (13) (2020) 5116–5126. doi:10.1021/acs.macromol.0c00577.
[24] K. Cui, Y. N. Ye, C. Yu, X. Li, T. Kurokawa, J. P. Gong, Stress Relaxation and Underlying Structure Evolution in Tough and Self-Healing Hydrogels, ACS Macro Letters 9 (11) (2020) 1582–1589. doi:10.1021/acsmacrolett.0c00600.
[25] X. Li, K. Cui, T. L. Sun, L. Meng, C. Yu, L. Li, C. Creton, T. Kurokawa, J. P. Gong, Mesoscale bicontinuous networks in self-healing hydrogels delay fatigue fracture 117 (14) (2020) 7606–7612. doi:10.1073/pnas.2000189117.
[26] A. B. Ihsan, T. L. Sun, T. Kurokawa, S. N. Karobi, T. Nakajima, T. Nonoyama, C. K. Roy, F. Luo, J. P. Gong, Self-Healing Behaviors of Tough Polyampholyte Hydrogels, Macromolecules 49 (11) (2016) 4245–4252. doi:10.1021/acs.macromol.6b00437.
[27] C.-J. Tsai, Y.-R. Chang, D.-J. Lee, Shape Stable Poly(vinyl alcohol) and Alginate Cross-Linked Hydrogel under Drying-Rewetting Cycles: Boron Substitution, Industrial & Engineering Chemistry Research 57 (42) (2018) 14213–14222. doi:10.1021/acs.iecr.8b03420.

[28] J. Thomas, K. Gomes, A. Lowman, M. Marcolongo, The effect of dehydration history on PVA/PVP hydrogels for nucleus pulposus replacement, Journal of Biomedical Materials Research Part B: Applied Biomaterials 69B (2) (2004) 135–140. doi:https://doi.org/10.1002/jbm.b.20023.

[29] S.-Y. Lee, B. P. Pereira, N. Yusof, L. Selvaratnam, Z. Yu, A. A. Abbas, T. Kamarul, Unconfined compression properties of a porous poly(vinyl alcohol)–chitosan-based hydrogel after hydration, Acta Biomaterialia 5 (6) (2009) 1919–1925. doi:10.1016/j.actbio.2009.02.014.
URL https://dx.doi.org/10.1016/j.actbio.2009.02.014

[30] M. Y. Truong, N. K. Dutta, N. R. Choudhury, M. Kim, C. M. Elvin, K. M. Nairn, A. J. Hill, The effect of hydration on molecular chain mobility and the viscoelastic behavior of resilin-mimetic protein-based hydrogels, Biomaterials 32 (33) (2011) 8462–8473. doi:10.1016/j.biomaterials.2011.07.064.
URL https://dx.doi.org/10.1016/j.biomaterials.2011.07.064

[31] X. Gao, W. Gu, A new constitutive model for hydration-dependent mechanical properties in biological soft tissues and hydrogels, Journal of Biomechanics 47 (12) (2014) 3196–3200. doi:https://doi.org/10.1016/j.jbiomech.2014.06.012.

[32] M. Smyth, M.-S. M'Bengue, M. Terrien, C. Picart, J. Bras, E. J. Foster, The effect of hydration on the material and mechanical properties of cellulose nanocrystal-alginate composites, Carbohydrate Polymers 179 (2018) 186–195. doi:https://doi.org/10.1016/j.carbpol.2017.09.002.

[33] X. N. Zhang, Y. J. Wang, S. Sun, L. Hou, P. Wu, Z. L. Wu, Q. Zheng, A Tough and Stiff Hydrogel with Tunable Water Content and Mechanical Properties Based on the Synergistic Effect of Hydrogen Bonding and Hydrophobic Interaction, Macromolecules 51 (20) (2018) 8136–8146. doi:10.1021/acs.macromol.8b01496.

[34] L. Li, L. Ren, L. Wang, S. Liu, Y. Zhang, L. Tang, Y. Wang, Effect of water state and polymer chain motion on the mechanical properties of a bacterial cellulose and polyvinyl alcohol (BC/PVA) hydrogel, RSC Adv. 5 (32) (2015) 25525–25531. doi:10.1039/C4RA11594E.

[35] G. I. Olivas, G. V. Barbosa-Cánovas, Alginate–calcium films: Water vapor permeability and mechanical properties as affected by plasticizer and relative humidity, LWT - Food Science and Technology 41 (2) (2008) 359–366. doi:https://doi.org/10.1016/j.lwt.2007.02.015.

[36] R. Pereira, A. Carvalho, D. C. Vaz, M. H. Gil, A. Mendes, P. Bártolo, Development of novel alginate based hydrogel films for wound healing applications, International Journal of Biological Macromolecules 52 (2013) 221–230. doi:https://doi.org/10.1016/j.ijbiomac.2012.09.031.

[37] R. Long, K. Mayumi, C. Creton, T. Narita, C.-Y. Hui, Time Dependent Behavior of a Dual Cross-Link Self-Healing Gel: Theory and Experiments, Macromolecules 47 (20) (2014) 7243–7250. doi:10.1021/ma501290h.
URL https://dx.doi.org/10.1021/ma501290h

[38] J. Guo, R. Long, K. Mayumi, C.-Y. Hui, Mechanics of a Dual Cross-Link Gel with Dynamic Bonds: Steady State Kinetics and Large Deformation Effects, Macromolecules 49 (9) (2016) 3497–3507. doi:10.1021/acs.macromol.6b00421.
URL https://dx.doi.org/10.1021/acs.macromol.6b00421

[39] M. Liu, J. Guo, C.-Y. Hui, C. Creton, T. Narita, A. Zehnder, Time-temperature equivalence in a PVA dual cross-link self-healing hydrogel, Journal of Rheology 62 (4) (2018) 991–1000. doi:10.1122/1.5029466.
URL https://dx.doi.org/10.1122/1.5029466

[40] R. Meacham, M. Liu, J. Guo, A. T. Zehnder, C. Y. Hui, Effect of Hydration on Tensile Response of a Dual Cross-linked PVA Hydrogel, Experimental Mechanics 60 (8) (2020) 1161–1165. doi:10.1007/s11340-020-00598-1.
URL https://dx.doi.org/10.1007/s11340-020-00598-1

[41] M. Liu, J. Guo, C.-Y. Hui, A. Zehnder, Crack tip stress based kinetic fracture model of a PVA dual-crosslink hydrogel, Extreme Mechanics Letters 29 (2019) 100457–100457. doi:10.1016/j.eml.2019.100457.
URL https://dx.doi.org/10.1016/j.eml.2019.100457

[42] J. Wang, T. Li, F. Cui, C.-Y. Hui, J. Yeo, A. T. Zehnder, Metamodeling of Constitutive Model Using

Gaussian Process Machine Learning, Submitted to Journal of the Mechanics and Physics of Solids (2021).

May 12, 2021